Talanta 201 (2019) 126–133

Contents lists available at ScienceDirect

Talanta

journal homepage: www.elsevier.com/locate/talanta

A portable and universal upconversion nanoparticle-based lateral flow assay platform for point-of-care testing

Yan Gong[a,b,1], Yamin Zheng[a,b,1], Birui Jin[a,b], Minli You[a,b], Jiayu Wang[a,b], XiuJun Li[c], Min Lin[a,b], Feng Xu[a,b], Fei Li[a,b,*]

[a] The Key Laboratory of Biomedical Information Engineering of Ministry of Education, School of Life Science and Technology, Xi'an Jiaotong University, Xi'an, PR China
[b] Bioinspired Engineering and Biomechanics Center (BEBC), Xi'an Jiaotong University, Xi'an, PR China
[c] Department of Chemistry and Biochemistry, Biomedical Engineering, Border Biomedical Research Center, Environmental Science and Engineering, University of Texas at El Paso, 500 West University Avenue, El Paso, TX, 79968, United States

ARTICLE INFO

Keywords:
UCNP-based biosensor
Point-of-care diagnostics
Paper microfluidics
Miniaturized device
Multiplexed detection
Telemedicine

ABSTRACT

Upconversion nanoparticle-based lateral flow assays (UCNP-LFAs) have attracted significant attention in point-of-care testing (POCT) applications, due to the long-term photostability and enhanced signal-to-background noise ratio. The existing UCNP-LFAs generally require peripheral equipment for exciting fluorescent signals and reading out fluorescence results, which are generally bulky and expensive. Herein, we developed a miniaturized and portable UCNP-LFA platform, which is composed of a LFA detection system, an UCNP-LFA reader and a smartphone-assisted UCNP-LFA analyzer. The LFA detection system is based on three types of UCNPs for multiplexed detection. The reader has a dimension of 24.0 cm × 9.4 cm × 5.4 cm (L × W × H) and weight of 0.9 kg. The analyzer based on the custom-designed software of a smartphone (termed as UCNP-LFA analyzer) can get the quantitative analysis results in a real-time manner. We demonstrated the universality of this platform by highly sensitive and quantitative detections of several kinds of targets, including small molecule (ochratoxin A, OTA), heavy metal ion (Hg^{2+}), bacteria (salmonella, SE), nucleic acid (hepatitis B virus, HBV) and protein (growth stimulation expressed gene 2, ST-2). Our developed UCNP-LFA platform holds great promise for applications in disease diagnostics, environmental pollution monitoring and food safety at the point of care.

1. Introduction

Public healthcare issues (*e.g.*, disease diagnostics, environmental monitoring and food safety testing) have attracted significant increasing attention worldwide, where there is an urgent need of point-of-care testing (POCT) technologies [1–4]. Most commercially available POCT technologies center around lateral flow assays (LFAs), where gold nanoparticles (GNPs) are routinely used as the report particles [5,6]. However, the GNP-based LFAs are associated with the issues of poor detection sensitivity and insufficient quantification capability due to the physical properties of GNPs [7–10]. To address these, various fluorophores (*e.g.*, quantum dots (QDs), fluorescence dyes) have been used to replace GNPs as the report particles in LFAs [11–13]. However, the fluorescent labels are normally excited by UV light, involving the drawbacks of strong background signal and the potential damage to the sample targets (especially biological samples) [14,15]. Besides, the fluorescence dyes are associated with the issue of photobleaching and instability during storage at ambient temperature [16,17]. Upconversion nanoparticles (UCNPs), as novel fluorescent nanoparticles with the properties of long-term photostability and negligible background signal, hold great promise in POCT applications [18,19], which when combined with LFAs (*i.e.*, UCNP-LFAs) offers robust photostability, enhanced signal-to-noise ratio and highly sensitive detection of various samples [20,21]. For example, in our previous work [22], we have developed the UCNP-LFAs and successfully applied them to sensitively detect several targets in food safety and environmental pollution monitoring fields. Thus, the UCNP-LFAs have found widespread POCT applications.

Generally, the UCNP-LFAs require peripheral equipment for exciting fluorescent signals and reading out fluorescence results of UCNPs [23]. To meet the requirement of POCT applications, the ideal UCNP-LFAs platforms should be portable with the capability of multiplexed

* Corresponding author. The Key Laboratory of Biomedical Information Engineering of Ministry of Education, School of Life Science and Technology, Xi'an Jiaotong University, Xi'an, PR China.
E-mail address: feili@mail.xjtu.edu.cn (F. Li).
[1] These authors contributed equally to this work.

https://doi.org/10.1016/j.talanta.2019.03.105
Received 9 January 2019; Received in revised form 24 March 2019; Accepted 30 March 2019
Available online 03 April 2019
0039-9140/

detection and universal for analysis of various samples, such as proteins, nucleic acids, heavy metal ions, bacteria and small molecules [24–26]. At present, the UCNP-LFAs equipment is mainly divided into the dynamic scanning type and the static imaging type according to the optical mechanism. The existing commercial equipment, such as Packard FluoroCount™ [27], UP*link*™ [28], and UPT-3A [29], all belong to the dynamic scanning type, which are neither portable nor convenient for the application scenario of POCT. For instance, the Packard FluoroCount™ needs an external IR laser (980 nm) to excite UCNPs and software in a computer to complete the data analysis (*e.g.*, background correction and peak-area determination) [15,27]. The UP*link*™ with built-in infrared laser and analysis software can only detect clinical samples of oral fluids in a qualitative manner (*e.g.*, positive, negative or invalid), which narrows its applications [28,30]. Although the UPT-3A has smaller size (33 cm × 20 cm × 20 cm (L × W × H)) and lighter weight than the above-mentioned two equipment, it is still not portable enough for the POCT applications. Compared to the dynamic scanning typed-equipment, the static imaging equipment for UCNP-LFAs is more cost-effective, time-saving and portable, thus more suitable for POCT [31,32]. Besides, it is possible to integrate smartphone with static imaging type, which makes the equipment more suitable for real-time and quantitative detection. Therefore, an inexpensive, compact, universal and user-friendly handheld platform is desired for commercialized applications of UCNP-LFAs in POCT.

In this study, we developed a miniaturized and portable UCNP-LFA platform (Fig. 1), which is composed of a LFA detection system, a smartphone-assisted UCNP-LFA reader and an analysis App (terms as UCNP-LFA App). In the platform, the LFA detection system is based on three types of UCNPs for multiplexed detection. The UCNP-LFA reader possesses the dimension of 24.0 cm × 9.4 cm × 5.4 cm (L × W × H) and weight of 0.9 kg. The custom-designed UCNP-LFA App can get the results in a real-time manner and the correlation coefficients over 0.992 compared with the gold-standard method [32]. The capability of this platform for highly sensitive and quantitative detections of different kinds of targets involved in public health, including nucleic acid (hepatitis B virus, HBV), protein (growth stimulation expressed gene 2, ST-2), small molecule (ochratoxin A, OTA), heavy metal ion (Hg^{2+}) and bacteria (salmonella, SE), has been demonstrated. The developed UCNP-LFA platform would be a powerful and universal POCT platform for quantitative detection of a variety of analytes for disease diagnostics, environmental pollution monitoring and food safety testing.

2. Experimental section

2.1. Chemicals and materials

$ErCl_3{\cdot}6H_2O$, $TmCl_3{\cdot}6H_2O$, $YbCl_3{\cdot}6H_2O$, $YCl_3{\cdot}6H_2O$, ammonium fluoride (NH_4F), EDC and poly (acrylic acid) (PAA) were all obtained from Sigma-Aldrich. Oleic acid and 1-octadecene were purchased from Alfa Aesar. Sulfo-NHS was obtained from Shanghai Gongjia Chemical Reagen Co., Ltd.. Diethylene glycol, methanol, cyclohexane, ethanol, sodium hydroxide and 2-(N-morpholino) ethanesulfonic acid (MES) were supplied by Tianjin Zhiyuan Chemical Reagent Co., Ltd.. The sequences of OTA, Hg^{2+}, SE-specified aptamers, human immunodeficiency virus (HIV), hepatitis C virus (HCV) and HBV probes designed according to the literature [10,33–38] were obtained from Shanghai Sangon Biotechnology Co., Ltd.. OTA was obtained from Dalian Meilun Biological Technology Co., Ltd.. Mercuric nitrate was supplied by Jiangsu Taixing Chemical Reagent Co., Ltd.. ST-2 antigen and antibodies were obtained from R&D Systems. B-type natriuretic peptide (BNP), C reactive protein (CRP), myoprotein (Myo) and N-terminal B-type natriuretic peptide (NT-proBNP) antigens were purchased from Fapon Biotech Co., Ltd.. Goat anti-mouse IgG was supplied by Guangzhou Green Biotechnology Co. Ltd.. All the components for preparation of LFA strips, including plastic adhesive backing pad, wicking pad, conjugate pad, sample pad and nitrocellulose (NC) membrane, were all obtained from Jiening Biotech Co., Ltd.. All the reagents employed in this work were analytical reagent grade. Aqueous solutions were prepared with ultrapure water (> 18 MΩ cm) from Barnstead Nanopure ultrapure water purification system (Thermo Fisher Scientific).

2.2. Synthesis of UCNPs

The green colored-core UCNPs (NaYF4:Yb/Er) used in this work were synthesized by a thermal decomposition procedure following our previous reports [32,39]. Briefly, $ErCl_3{\cdot}6H_2O$ (0.02 mmol), $YCl_3{\cdot}6H_2O$ (0.8 mmol) and $YbCl_3{\cdot}6H_2O$ (0.18 mmol) were dissolved in a flask containing 10 mL 1-octadecene and 5 mL oleic acid. Then the mixture was stirred at room temperature for 20 min, heated to 118 °C for 1.5 h under nitrogen atmosphere and followed by 166 °C for another 2 h to remove water. After cooling down to room temperature, 5 mL methanol solution containing 4% NaOH and 6% NH_4F was added to the above solution and remained stirring at room temperature overnight. Then the

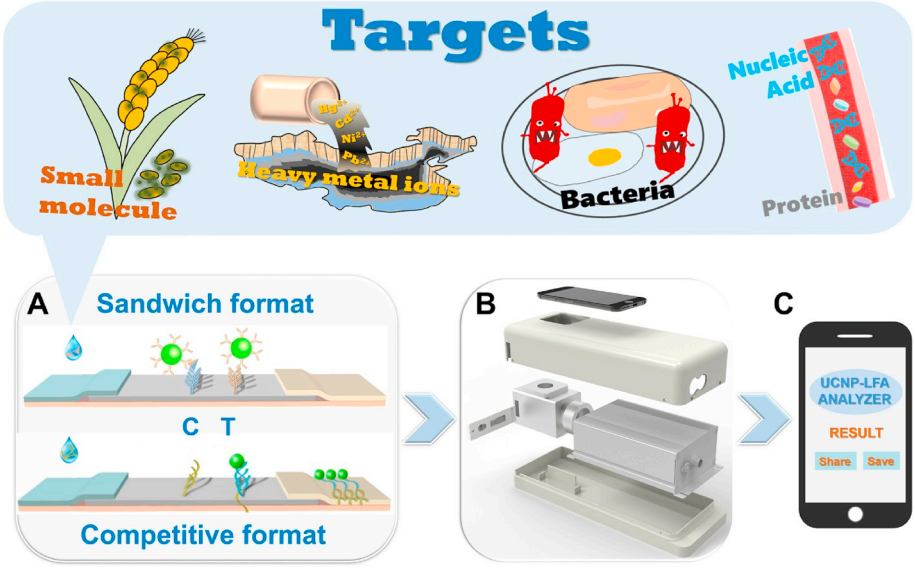

Fig. 1. Schematic diagram of the UCNP-LFA platform. (A) LFA detection system; (B) UCNP-LFA reader and (C) UCNP-LFA App.

reaction mixture was heated to 300 °C and kept for 2 h until cooling down to room temperature. The resulting products of $NaYF_4$:Yb/Er were centrifuged and washed with 5 mL cyclohexane and 10 mL ethanol for three times, and finally dispersed in 5 mL cyclohexane. To synthesize the core-shell UCNPs ($NaYF_4$:Yb/Er@$NaYF_4$), the same procedure was performed with only changing the amount of $YCl_3{\cdot}6H_2O$ to 0.5 mmol, and adding the as-prepared $NaYF_4$:Yb/Er solution into the reaction solution before adding methanol solution of NH_4F and NaOH. The size distributions and fluorescence intensities of the as-prepared UCNPs were characterized by transmission electron microscopy (TEM, JEM-2100F) and fluorescence spectrophotometer (QuantaMaster TM40), respectively.

2.3. Surface modification of UCNPs

The surface modification of UCNPs was carried out with using PAA as a multi-dentate ligand to displace the hydrophobic ligands on the UCNPs surface to make them water soluble based on a ligand exchange process. Briefly, 1 mL UCNPs solution was centrifuged and re-dispersed in 2 mL chloroform (~15 mg/mL), then stirred with 0.0158 g PAA and 2 mL ethanol for 24 h. And the products were centrifuged and washed with ethanol twice and re-dispersed in 5 mL PBS solution.

2.4. Preparation of UCNP probes

There are two types of UCNP probes used in this work, *i.e.*, the UCNP-DNA probe and the UCNP-antibody probe. In the preparation of UCNP-DNA probe, 200 μL of the above prepared UCNPs@PAA solution was centrifuged and re-suspended in 200 μL MES buffer. Then 12 μL of 10 mM sulfo-NHS and 24 μL of 10 mM EDC were successively added into the above solution and activated at 37 °C for 2 h. 160 μL of 2 μM DNA was added to the above solution and incubated for 24 h. The UCNP-DNA conjugation was centrifuged and washed with PBS for four times and finally suspended in 200 μL Tris-HCl buffer. For the preparation of UCNP-antibody probe, 6 μL of 30 mM sulfo-NHS and EDC were successively added into 200 μL of UCNPs@PAA solution for activation for 0.5 h at room temperature. The activated products were washed with MES buffer for three times and re-dispersed in 200 μL MES buffer. Then 5 μg antibodies were added into 200 μL re-dispersed MES solution and incubated for 2 h. After that, 6 μL of 2 M glycine stop buffer was added. The UCNP-antibody conjugation was washed with storage buffer (0.1% NaN_3, 50 mM glycine, 0.03% v/v triton) for three times and finally dissolved in 200 μL storage buffer and stored at 4 °C before use.

2.5. Preparation of UCNP-LFAs

The UCNP-LFAs were fabricated according to the previous protocol [7]. Briefly, the sample pad, conjugate pad, NC membrane and wicking pad were successively mounted on an adhesive backing pad with 1-2 mm overlap between two adjoining pads. The following processes were then performed before assembling the UCNP-based strip. First, the as-prepared UCNP probes were diluted by eluent buffer (pH 8.18, containing 0.85% [w/v] Tris, 1% [w/v] BSA and 10% [w/v] sucrose) before being dispensed on the conjugate pad at 40 μL/cm. Second, the control and test lines were fabricated by dispersing corresponding control probe and capture probe through Dispenser HM3030 (Goldbio Co., China) according to the sample to be tested. Then the obtained conjugate pad and NC membrane were dried in an oven at 37 °C for 2 h. Finally, the above pads were assembled and cut into strips (3.0 mm) by Matrix™ Programmable Sheer (Kinematic Automation, USA). The strips were separately put into the plastic cartridges with two windows, *i.e.*, the result detecting window and the sample adding window.

2.6. Operation procedure with the fabricated UCNP-LFAs

After introducing the specimen into the sample adding window of the fabricated LFAs for 15 min, the strip was inserted into the UCNP-LFA reader and detected by the smartphone. The photographs of the detection results were analyzed using our custom-designed App to calculate the optical density of test line (T) and background (B). The difference between "T" and "B" values is proportional to the concentration of the target analytes. Through detecting a series of samples with standard concentrations, a working curve between "T vs. B" values and the concentration of target analyte can be fitted as the detecting rule of the UCNP-LFA App. Then the unknown concentration of sample can be calculated through the App. The detection results displayed on the smartphone interface can be further uploaded to the cloud for telemedicine of users. Besides, we performed the correlation analysis between our UCNP-LFA platform and the gold-standard method in lab. The detailed operation procedures of our UCNP-LFA platform and the gold-standard method are described as follows: to use the portable reader/benchtop NIR-CW-laser (Changchun Liangli Photoelectric Co., Ltd.) to excite UCNPs of the detected strips, smartphone/Nikon D90 single-lens reflex camera to obtain fluorescence photos, UCNP-LFA App/computer software to analyze the signal values. Then the correlation coefficients between these two groups of signal values were calculated.

2.7. Characterization of the UCNP-LFA reader

The spectrum of the laser diode was tested by an optical spectrum analyzer (Yokogawa, AQ6370). The characterization of the transmittance curves of the infrared filter and the dichroic mirror were both performed by a spectrometer (Princeton Instruments, SpectraPro 2500i).

3. Results and discussion

3.1. Morphology and fluorescence intensity of the as-prepared UCNPs

The morphology, size distribution and fluorescence intensity of the as-prepared UCNPs have significant effects on their detection performance used in UCNP-LFAs. First, we utilized TEM to characterize the morphology and size distribution of the as-prepared core and core-shell UCNPs. From the obtained TEM images of UCNPs in Fig. S1 (Supporting Information), the morphology of the bare core UCNPs and the core-shell UCNPs present uniform hexagon shape. The average sizes of bare core UCNPs and core-shell UCNPs are found to be ~67 nm and ~109 nm, respectively. The thickness of the shell layer on the core UCNPs is found to be ~ 21 nm. Second, the fluorescence intensity of the as-prepared UCNPs was characterized by fluorescence measurement. From the recorded fluorescence emission spectrum of the core and core-shell UCNPs in Fig. S2 (Supporting Information), we can observe that the core-shell UCNPs possess about six times enhancement of fluorescence intensity than that of the bare core UCNPs, which can be contributed to the inhibition of shell structure to surface passivation effect of core. Moreover, we can find that the both core and core-shell UCNPs display green emission at peak of 540 nm, which can be used as an index parameter to choose the infrared filter for the following UCNP-LFA platform.

3.2. Design of the UCNP-LFA detection system

As shown in Fig. 1, the structure of the portable UCNP-LFA platform is composed of a LFA detection system (Fig. 1A), a smartphone-assisted UCNP-LFA reader (Fig. 1B) and an UCNP-LFA App (Fig. 1C). The fabricated UCNP-LFA platform has dimension of 24.0 cm × 9.4 cm × 5.4 cm (L × W × H) and weight of 0.9 kg (Fig. 2A). The significantly miniaturized size and weight of the platform compared to the existing

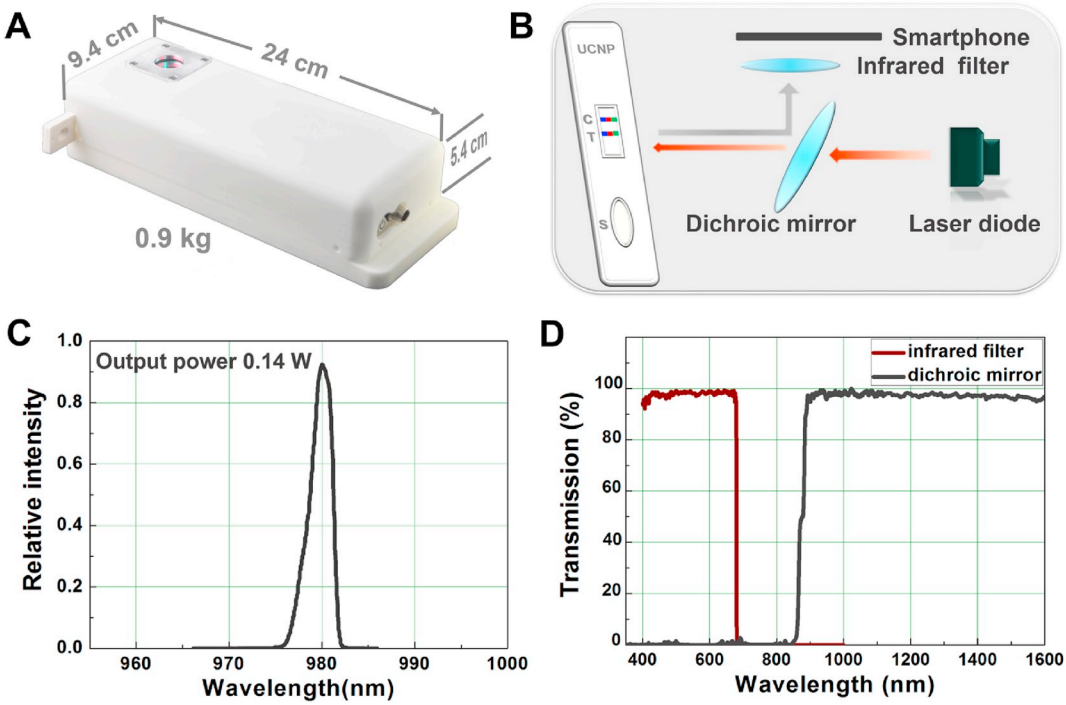

Fig. 2. Characterization results of the optical system of the UCNP-LFA reader. (A) Photograph of the UCNP-LFA reader. (B) Schematic diagram of the UCNP-LFA reader. (C) Spectrum of the laser diode with central wavelength of 980 nm at 0.14 W. (D) Spectral transmission curves of the infrared filter and the dichroic mirror.

equipment make it more portable and adopted for POCT applications.

Five different UCNP-LFAs, including HBV-UC-LFA for nucleic acid (HBV), ST2-UC-LFA for proteins (ST-2), OTA-UC-LFA for small molecule (OTA), Hg^{2+}-UC-LFA for heavy metal ion (Hg^{2+}) and SE-UC-LFA for bacteria (SE), were prepared and used to testify our platform. Among the five UCNP-LFAs, the work principles of HBV-UC-LFA and ST2-UC-LFA are based on the sandwich format. That is, if there is a detection target in the sample, the UCNP probes firstly react with the target. The conjugates are then recognized by the target-specified capture probes at the test line, and the excess free UCNP probes are captured at the control line. With increasing the amount of targets in the sample, more UCNP probes will accumulate in the test line, leading to the increased fluorescent signal of the test line (*i.e.*, "T" signal). For the Hg^{2+}-UC-LFA, SE-UC-LFA and OTA-UC-LFA, the competitive format is used, as demonstrated in our previous work [22]. That is, when there are targets present in the sample, the UCNP probes firstly react with the targets and the free UCNP probes without reaction with targets will be captured by the test line. With increasing amount of targets in the sample, fewer UCNP probes will accumulate in the test line, resulting in the decreased fluorescent "T" signal (Fig. 1B). Then the quantitative detections of targets can be achieved through reading the fluorescent signal difference between "T" and background values using our developed UCNP-LFA reader and App. The details of the detection performances of the developed HBV-UC-LFAs and ST2-UC-LFAs, including the limit of detection (LOD), repeatability, specificity and validity in spiked-serum samples, are demonstrated in Supporting Information.

3.3. Structure and performance of the UCNP-LFA reader

The structure of the UCNP-LFA reader is shown in Fig. 2B, in which a compact and small infrared laser is applied to excite UCNPs on the NC membrane, a dichroic mirror placed at 45-degree angle with a horizontal plane transmits infrared laser and reflects visible luminescence, and an infrared filter placed right under the camera of the smartphone decreases the interference of the residual excitation light. To ensure good imaging results and high detection sensitivity, the follow aspects have been considered during the reader design. First, to achieve the maximized fluorescence excitation and thus the increase of the detection sensitivity, the central wavelength of the laser diode is highly consistent with the excitation wavelength of the UCNPs used in LFAs. Second, the spot size of the laser diode covers the detection area of NC membrane to ensure the accuracy of the imaging results. Third, the dichroic mirror has ultrahigh infrared transmission and high reflectivity of visible light, the infrared filter has a great cut-off efficiency to the laser and high transmittance at the emitted light wavelength, which can greatly reduce the background and noise through eliminating the stray light.

The performance of the UCNP-LFA reader was evaluated through the following steps. First, we tested the spectrum of the laser diode. As shown in Fig. 2C, a central wavelength of 980 nm of the laser diode, which can completely excite the trapped UCNPs in the test line of LFAs and then result in their maximum emission, is obtained. From the transmittance curves of the dichroic mirror and the filter (Fig. 2D), we can observe that the transmission of the dichroic mirror is about 98% at 980 nm and approaches 0 at visible spectrum, indicating that the dichroic filter possesses excellent transmittance at the excitation wavelength and super high reflection in the region of visible light. The transmission of the infrared filter is more than 95% between 400 and 679 nm and approaches 0 at 980 nm, indicating that the infrared filter can completely block the laser light but with high transmittance at the emitted light wavelength. Through the above design, we can reduce the interference of miscellaneous lights and the laser energy loss at the greatest extent, thus enhancing the detection sensitivity and accuracy of the UCNP-LFA platform.

3.4. Results analysis procedure using the UCNP-LFA App

In the analysis system of the UCNP-LFA platform, the fluorescent signal emitted by UCNPs on the NC membrane of LFAs can be captured by the camera of a smartphone and then be converted to the sample concentration by the UCNP-LFA App in a real-time manner, which can interact with telemedicine. As illustrated in Fig. 3 and the operation video in Supporting Information, after inserting the UCNP-LFA into the

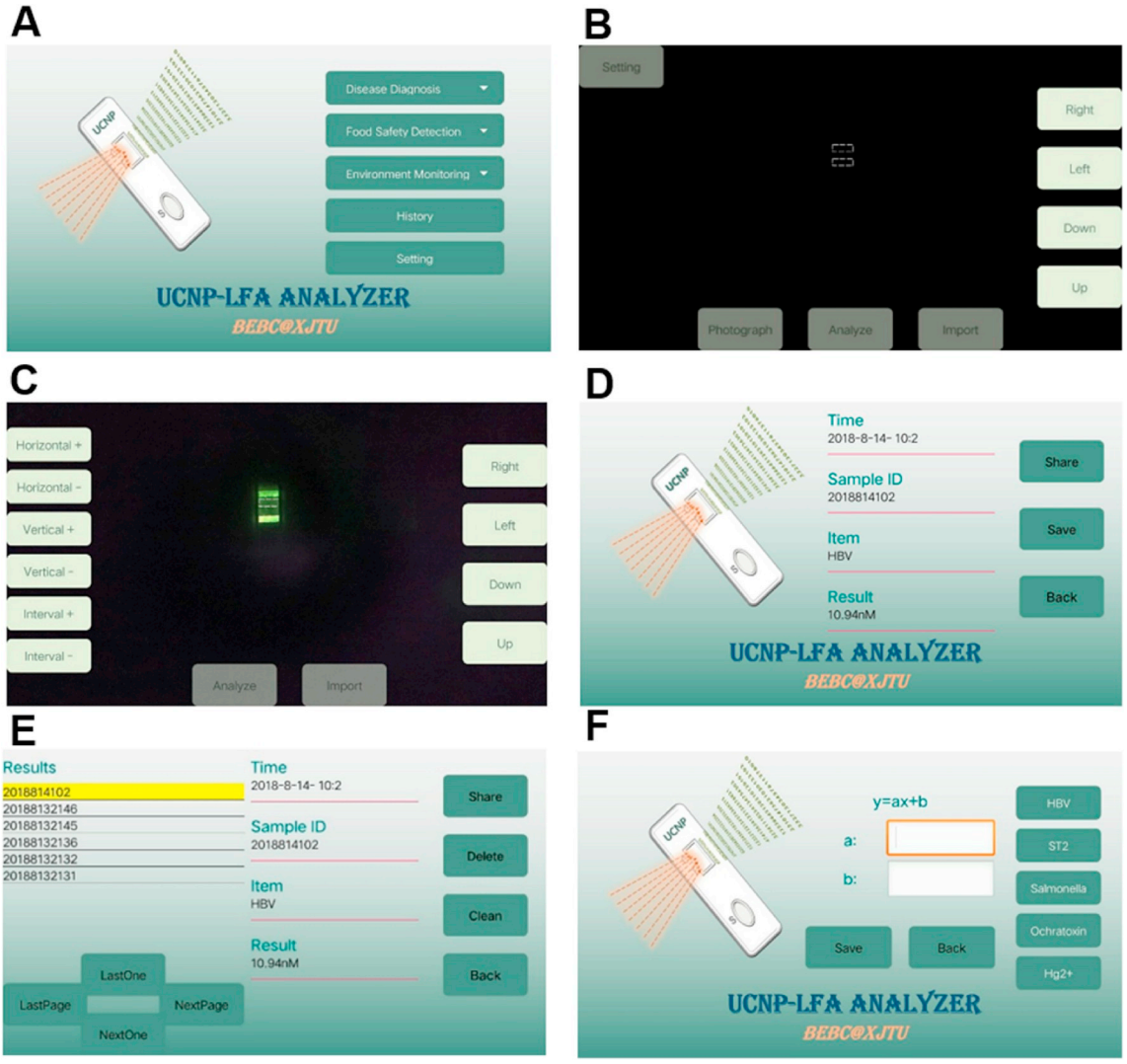

Fig. 3. Operation procedure of the UCNP-LFA App. (A) The initial interface; (B-C) the analysis page; (D) the result page; (E) the history page and (F) the setting page of the UCNP-LFA App.

reader, the users run UCNP-LFA App on the smartphone and click different operation columns to start test items (Fig. 3A). Among them, "Disease Diagnosis" represents the ST-2 detection for heart failure prognosis and HBV detection, "Food Safety Detection" represents OTA and SE detections, and "Environment Monitoring" is for Hg^{2+} detection. After selecting the test items, images are captured by the camera of the smartphone via clicking the "Photograph" button or imported from photo library stored in smartphone by clicking the "Import" button (Fig. 3B), which can be saved as bitmap format with 32-bit images. Via "Setting" and the other four buttons on the right side of the screen (Fig. 3C), users can adjust the size of the recognition box and the interval between these two boxes, and move the recognition box to match the background and test line of the LFA, ensuring the precise identification of the detection results. After clicking the button "Analyze", the RGB value can be extracted from the selected area, and the difference of RGB value between the test line and the background can be substituted into the calibration curve for calculation. Then all the steps are automatically implemented by a simple built-in algorithms of the software, and the concentration of target analytes can be finally reported on the screen of smartphone (Fig. 3D), which can also be saved in the smartphone or shared through internet via email, message, Wechat and telemedicine network. At the same time, on the UCNP-LFA App, users can review the results via "History", where all the previous detection data of the test items are stored (Fig. 3E), and revise the calibration curve to a new test by clicking the "Setting" button on the main menu (Fig. 3F). The UCNP-LFA App can accomplish five-item analysis, three-color extraction and two kinds of shape recognition. The simple and fool-style operation advantage also extend the applications of the UCNP-LFA platform for various users.

Supplementary video related to this article can be found at https://doi.org/10.1016/j.talanta.2019.03.105

3.5. Detection results of nucleic acid using the UCNP-LFA platform

The HBV-UC-LFAs were used to detect hepatitis B virus nucleic acid through the nucleic acid hybridization method. As shown in Fig. 4A,B, the fluorescence intensities of the test lines increase with the increase of the HBV concentration (0–10 nM). The quantification of the fluorescence intensities of HBV-UC-LFAs was further performed using both the gold-standard method and our UCNP-LFA platform. As shown in Fig. 4C, even the fluorescence intensities of the HBV-UC-LFAs recoded by our platform is lower compared to the gold-standard method due to the difference of the exposure between the camera and smartphone, the results of these two methods still maintain a good logarithmic relationship ($y = 13.282\ln(x) + 25.015$, $R^2 = 0.922$) between the HBV concentration (0–10 nM) and the signal intensity. To further evaluate

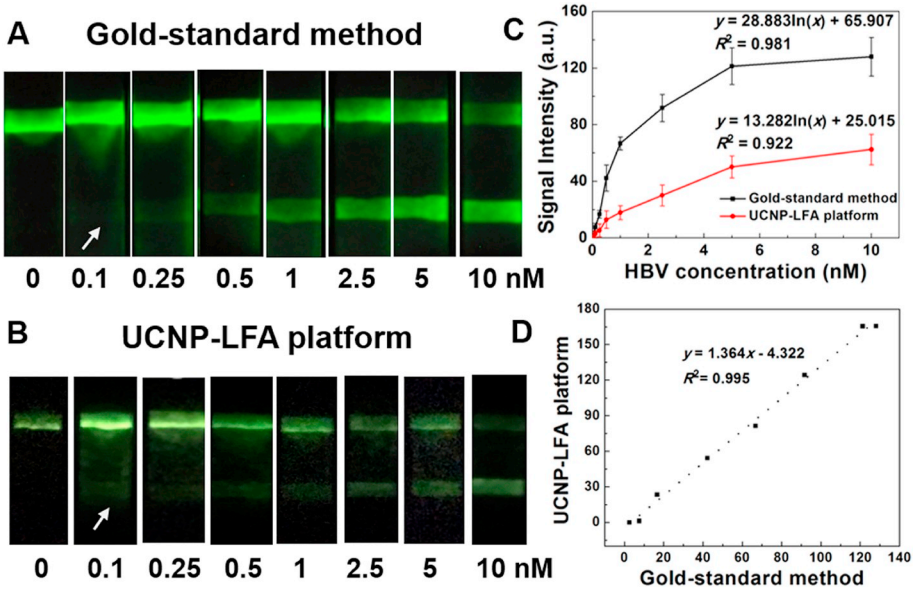

Fig. 4. Detection results of HBV using the gold-standard method and our developed UCNP-LFA platform. Photographs of UCNP-LFAs taken by (A) the gold-standard method and (B) the UCNP-LFA platform. (C) Standard working curve of HBV-UC-LFA with the above two methods. (D) Correlation of the detection results of HBV-UC-LFA using the gold-standard method and our UCNP-LFA platform. (For interpretation of the references to color in this figure legend, the reader is referred to the Web version of this article.)

the accuracy of our developed platform, we utilized both the gold-standard method and our UCNP-LFA platform to detect the HBV-UC-LFAs. From the correlation of the detection results using the two methods (Fig. 4D), we can get a good linear correlation ($y = 1.364x$ - 4.322) between the gold-standard method and our platform with the correlation coefficient of $R^2 = 0.995$. These results demonstrated the ability of our developed platform for quantitative detection of nucleic acids.

3.6. Detection results of protein using the UCNP-LFA platform

The ST2-UC-LFAs were utilized to detect ST-2 (a typical biomarker for diagnosis of heart failure) based on immunoreaction. From the obtained results in Fig. 5A and B, the fluorescence intensities of the test lines increase with the increase of the ST-2 concentration (0–250 ng/mL), and the quantification of them can be further confirmed. As shown in Fig. 5C, the fluorescence intensities of ST2-UC-LFAs recorded using our platform are lower compared with the gold-standard method because of the different exposure of the camera and smartphone, but the results of the two methods maintain a good logarithmic relationship ($y = 13.447\ln(x)$ - 11.290, $R^2 = 0.986$) between the ST-2 concentration (0–250 ng/mL) and the fluorescence intensity. The accuracy of our developed platform for detection of ST2-UC-LFAs was further evaluated with utilizing the gold-standard method and our UCNP-LFA reader and analysis App. From the correlation of the detection results in Fig. 5D, a good linear correlation ($y = 0.512x$ - 0.971) between the gold-standard method and our platform with the correlation coefficient of $R^2 = 0.992$ is obtained. These results demonstrate the capability of our developed platform for quantitative detection of biomarker (*e.g.*, protein).

3.7. Detection results of bacteria, heavy metal ion and small molecule using the UCNP-LFA platform

To further prove the widespread application of our developed platform for detecting more targets in POCT (*e.g.*, bacteria, heavy metal ions and small molecules), we selected SE, Hg^{2+} and OTA as the detecting model targets and used the UCNP-LFA platform to detect them. As shown in Fig. 6A,B, the fluorescence intensities of the test lines of these targets

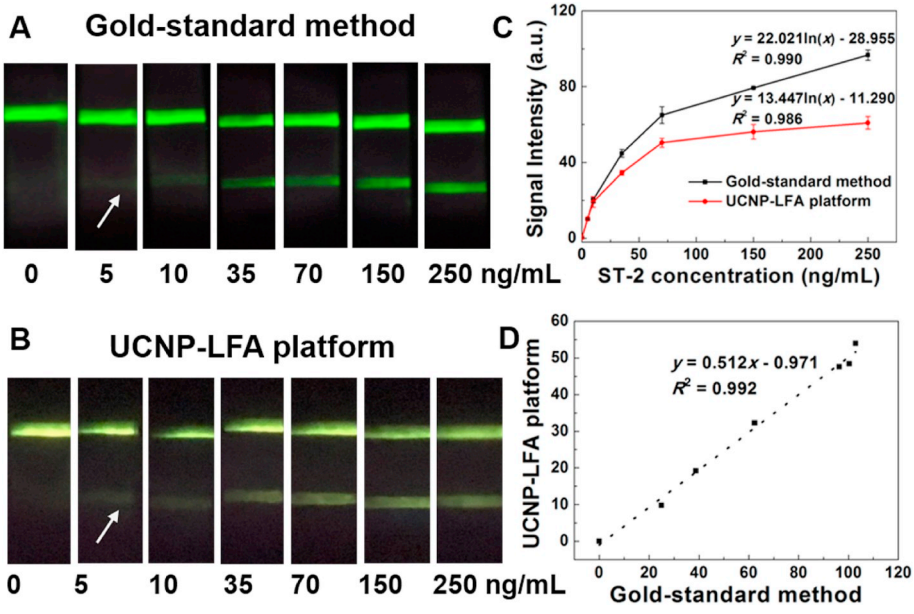

Fig. 5. Detection results of ST-2 using the gold-standard method and our developed UCNP-LFA platform. Photographs of UCNP-LFAs taken by (A) the gold-standard method and (B) the UCNP-LFA platform. (C) Standard working curve of ST2-UC-LFA with the above two methods. (D) Correlation of the detection results of ST2-UC-LFA using the gold-standard method and the UCNP-LFA platform. (For interpretation of the references to color in this figure legend, the reader is referred to the Web version of this article.)

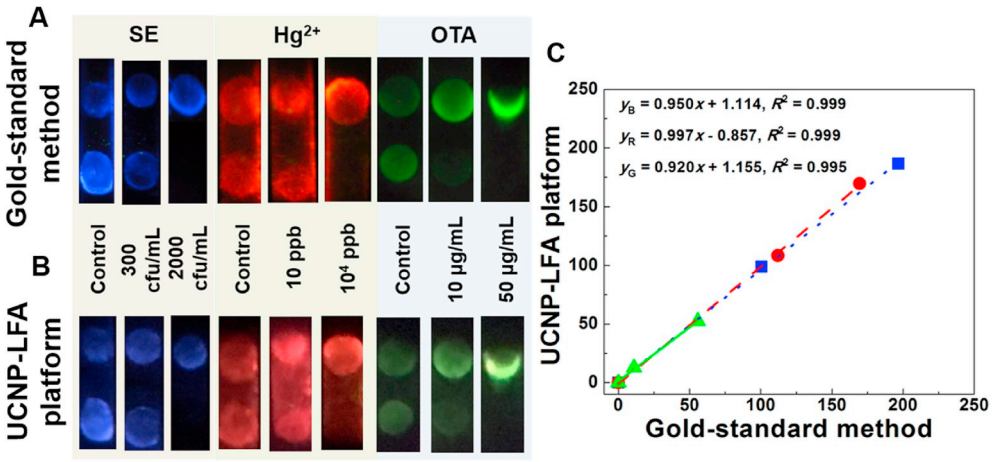

Fig. 6. Detection results of SE, Hg^{2+} and OTA using the gold-standard method and our developed UCNP-LFA platform. Photographs of UCNP-LFAs taken by (A) the gold-standard method and (B) the UCNP-LFA platform. (C) Correlation of the detection results of SE-UC-LFA, Hg^{2+}-UC-LFA and OTA-UC-LFA using the gold-standard method and the UCNP-LFA platform. (For interpretation of the references to color in this figure legend, the reader is referred to the Web version of this article.)

decrease with the increases of the target concentrations (from zero to high concentration). From the correlation of the detection results of our platform compared with the gold-standard method (Fig. 6C), we obtained the good linear correlations (SE: $y = 0.950x + 1.114$; Hg^{2+}: $y = 0.997x - 0.857$; OTA: $y = 0.920x + 1.155$) with the corresponding correlation coefficient of $R^2 = 0.999$, 0.999 and 0.995, respectively. The results demonstrate the capability and the advantage of our UCNP-LFA platform for quantitative detections of bacteria, heavy metal ions and small molecules.

4. Conclusions

In this work, we successfully developed a miniaturized and portable UCNP-LFAs-based POCT platform with dimension of 24.0 cm × 9.4 cm × 5.4 cm (L × W × H) and weight of 0.9 kg, which integrates a LFA detection system, a smartphone-assisted UCNP-LFA reader and a simple-operated analysis App. In the platform, the universality of UCNP-LFAs was identified by successfully detections of five kinds of targets (HBV, ST-2, OTA, Hg^{2+}, SE), which represent the typical nucleic acid, protein, small molecule, heavy metal ion and bacteria for disease diagnostics, environmental pollution monitoring and food safety testing in the POCT field. Based on the UCNP-LFA App, the precision and accuracy of the UCNP-LFAs platform are comparable to the gold-standard method with the correlation coefficients over 0.992. The highly sensitive and quantitative detection capability of the UCNP-LFAs platform meets the requirement of clinical testing, and their detection limit is lower by approximately 5–10 fold compared with the clinical cut-off value. The universality of UCNP-LFAs and minimization of its reader make the high sensitive and multiplex UCNP-LFAs-based POCT platform highly promising for commercialization and applications in disease diagnostics, environmental pollution monitoring and food safety testing.

Acknowledgments

This work was financially supported by the National Natural Science Foundation of China (21775117), the Key Program for Science and Technology Innovative Research Team in Shaanxi Province of China (2017KCT-22), the Program for Innovative Research Team in Yulin Shaanxi Province of China (2017KJJH-02), the High Level Returned Overseas Students Foundation ([2018]642) and the General Financial Grant from the China Postdoctoral Science Foundation (2016M592773).

Appendix A. Supplementary data

Supplementary data to this article can be found online at https://doi.org/10.1016/j.talanta.2019.03.105.

References

[1] P. Yager, G.J. Domingo, J. Gerdes, Point-of-care diagnostics for global health, Annu. Rev. Biomed. Eng. 10 (2008) 107–144.
[2] A.W. Martinez, S.T. Phillips, G.M. Whitesides, E. Carrilho, Diagnostics for the developing world: microfluidic paper-based analytical devices, Anal. Chem. 82 (2010) 3–10.
[3] J. Hu, L. Wang, F. Li, Y.L. Han, M. Lin, T.J. Lu, F. Xu, Oligonucleotide-linked gold nanoparticle aggregates for enhanced sensitivity in lateral flow assays, Lab Chip 13 (2013) 4352–4357.
[4] J.W. Shangguan, Y. Liu, S. Wang, Y.X. Hou, B.Y. Xu, J.J. Xu, H.Y. Chen, Paper capillary enables effective sampling for microfluidic paper analytical devices, ACS Sens. 3 (2018) 1416–1423.
[5] A.K. Yetisen, M.S. Akram, C.R. Lowe, Paper-based microfluidic point-of-care diagnostic devices, Lab Chip 13 (2013) 2210–2251.
[6] N.T.K. Thanh, Z. Rosenzweig, Development of an aggregation-based immunoassay for anti-protein A using gold nanoparticles, Anal. Chem. 74 (2002) 1624–1628.
[7] Y. Gong, J. Hu, J.R. Choi, M. You, Y. Zheng, B. Xu, T. Wen, F. Xu, Improved LFIAs for highly sensitive detection of BNP at point-of-care, Int. J. Nanomed. 12 (2017) 4455–4466.
[8] J. Hu, X. Cui, Y. Gong, X. Xu, B. Gao, T. Wen, T.J. Lu, F. Xu, Portable microfluidic and smartphone-based devices for monitoring of cardiovascular diseases at the point of care, Biotechnol. Adv. 34 (2016) 305–320.
[9] B. Liu, D. Du, X. Hua, X.Y. Yu, Y. Lin, Paper-based electrochemical biosensors: from test strips to paper-based microfluidics, Electroanalysis 26 (2014) 1214–1223.
[10] R. Tang, H. Yang, Y. Gong, Z. Liu, X.J. Li, T. Wen, Z.G. Qu, S. Zhang, Q. Mei, F. Xu, Improved analytical sensitivity of lateral flow assay using sponge for HBV nucleic acid detection, Sci. Rep. 7 (2017) 1360–1369.
[11] L. Wang, W. Chen, W. Ma, L. Liu, W. Ma, Y. Zhao, Y. Zhu, L. Xu, H. Kuang, C. Xu, Fluorescent strip sensor for rapid determination of toxins, Chem. Commun. 47 (2011) 1574–1576.
[12] Y. Xu, Y. Liu, Y. Wu, X. Xia, Y. Liao, Q. Li, Fluorescent probe-based lateral flow assay for multiplex nucleic acid detection, Anal. Chem. 86 (2014) 5611–5614.
[13] Q. You, M. Liu, Y. Liu, H. Zheng, Z. Hu, Y. Zhou, B. Wang, Lanthanide-labeled immunochromatographic strip assay for the on-site identification of ancient silk, ACS Sens. 2 (2017) 569–575.
[14] C. Liu, W. Ma, Z. Gao, J. Huang, Y. Hou, C. Xu, W. Yang, M. Gao, Upconversion luminescence nanoparticles-based lateral flow immunochromatographic assay for cephalexin detection, J. Mater. Chem. C 2 (2014) 9637–9642.
[15] R.S. Niedbala, H. Feindt, K. Kardos, T. Vail, J. Burton, B. Bielska, S. Li, D. Milunic, P. Bourdelle, R. Vallejo, Detection of analytes by immunoassay using up-converting phosphor technology, Anal. Biochem. 293 (2001) 22–30.
[16] Z. Zhang, D. Wang, J. Li, Q. Zhang, P.W. Li, Monoclonal antibody-europium conjugate-based lateral flow time-resolved fluoroimmunoassay for quantitative determination of T-2 toxin in cereals and feed, Anal. Methods 7 (2015) 2822–2829.
[17] Y. Chen, Q. Chen, M. Han, J. Liu, P. Zhao, L. He, Y. Zhang, Y. Niu, W. Yang, L. Zhang, Near-infrared fluorescence-based multiplex lateral flow immunoassay for the simultaneous detection of four antibiotic residue families in milk, Biosens. Bioelectron. 79 (2016) 430–434.
[18] S. Wilhelm, Perspectives for upconverting nanoparticles, ACS Nano 11 (2017) 10644–10653.
[19] Z. Luo, L. Zhang, R. Zeng, L. Su, D. Tang, Near-infrared light-excited core-core-shell UCNP@Au@CdS upconversion nanospheres for ultrasensitive photoelectrochemical enzyme immunoassay, Anal. Chem. 90 (2018) 9568–9575.
[20] G.J.V. Dam, C.J.D. Dood, M. Lewis, A.M. Deelder, L.V. Lieshout, H.J. Tanke, L.H.V. Rooyen, P.L.A.M. Corstjens, A robust dry reagent lateral flow assay for diagnosis of active schistosomiasis by detection of Schistosoma circulating anodic antigen, Exp. Parasitol. 135 (2013) 274–282.
[21] E. Juntunen, T. Salminen, S.M. Talha, I. Martiskainen, T. Soukka, K. Pettersson, M. Waris, Lateral flow immunoassay with upconverting nanoparticle-based detection for indirect measurement of interferon response by the level of MxA, J. Med.

Virol. 89 (2016) 598–605.
[22] B. Jin, Y. Yang, R. He, Y.I. Park, A. Lee, D. Bai, F. Li, T.J. Lu, F. Xu, M. Lin, Lateral flow aptamer assay integrated smartphone-based portable device for simultaneous detection of multiple targets using upconversion nanoparticles, Sens. Actuators, B 276 (2018) 48–56.
[23] Z. Yan, L. Zhou, Y. Zhao, J. Wang, L. Huang, K. Hu, H. Liu, H. Wang, Z. Guo, Y. Song, Rapid quantitative detection of Yersinia pestis by lateral-flow immunoassay and up-converting phosphor technology-based biosensor, Sens. Actuators, B 119 (2006) 656–663.
[24] W.G. Lee, Y.G. Kim, B.G. Chung, U. Demirci, A. Khademhosseini, Nano/Microfluidics for diagnosis of infectious diseases in developing countries, Adv. Drug Deliv. Rev. 62 (2010) 449–457.
[25] V. Gubala, L.F. Harris, A.J. Ricco, M.X. Tan, D.E. Williams, Point of care diagnostics: status and future, Anal. Chem. 84 (2012) 487–515.
[26] L. Gervais, R.N. De, E. Delamarche, Microfluidic chips for point-of-care immunodiagnostics, Adv. Mater. 23 (2011) H151–H176.
[27] P. Corstjens, M. Zuiderwijk, A. Brink, S. Li, H. Feindt, R.S. Niedbala, H. Tanke, Use of up-converting phosphor reporters in lateral-flow assays to detect specific nucleic acid sequences: a rapid, sensitive DNA test to identify human papillomavirus type 16 infection, Clin. Chem. 47 (2001) 1885–1893.
[28] V.K. Mokkapati, R. Sam Niedbala, K. Kardos, R.J. Perez, M. Guo, H.J. Tanke, P.L. Corstjens, Evaluation of UPlink–RSV, Ann. N. Y. Acad. Sci. 1098 (2007) 476–485.
[29] Y. Zhao, X. Liu, X. Wang, C. Sun, X. Wang, P. Zhang, J. Qiu, R. Yang, L. Zhou, Development and evaluation of an up-converting phosphor technology-based lateral flow assay for rapid and quantitative detection of aflatoxin B1 in crops, Talanta 161 (2016) 297–303.
[30] P.L. Corstjens, S. Li, M. Zuiderwijk, K. Kardos, W.R. Abrams, R.S. Niedbala, H.J. Tanke, Infrared up-converting phosphors for bioassays, IEE Proc. - Nanobiotechnol. 152 (2005) 64–72.
[31] L. Lei, Z. Lei, L. Huang, Z. Yan, Y. Zhao, R. Yang, A. Zeng, K. Yu, H. Huang, CCD-based detection system for immunity-chromatography test strip, Chin. J. Sci. Instrum. 28 (2007) 246–251.
[32] M. You, M. Lin, Y. Gong, S. Wang, A. Li, L. Ji, H. Zhao, K. Ling, T. Wen, Y. Huang, Household fluorescent lateral flow strip platform for sensitive and quantitative prognosis of heart failure using dual-color upconversion nanoparticles, ACS Nano 11 (2017) 6261.
[33] X. Ma, Y. Jiang, F. Jia, Y. Yu, J. Chen, Z. Wang, An aptamer-based electrochemical biosensor for the detection of Salmonella, J. Microbiol. Methods 98 (2014) 94–98.
[34] Q. Li, M. Michaelis, G. Wei, C.L. Colombi, A novel aptasensor based on single-molecule force spectroscopy for highly sensitive detection of mercury ions, Analyst 140 (2015) 5243–5250.
[35] J.A. Cruzaguado, G. Penner, Determination of ochratoxin a with a DNA aptamer, J. Agric. Food Chem. 56 (2008) 10456–10461.
[36] W. Ma, H. Yin, L. Xu, Z. Xu, H. Kuang, L. Wang, C. Xu, Femtogram ultrasensitive aptasensor for the detection of Ochratoxin A, Biosens. Bioelectron. 42 (2013) 545–549.
[37] H. Kuang, W. Chen, D. Xu, L. Xu, Y. Zhu, L. Liu, H. Chu, C. Peng, C. Xu, S. Zhu, Fabricated aptamer-based electrochemical "signal-off" sensor of ochratoxin A, Biosens. Bioelectron. 26 (2011) 710–716.
[38] H. Lee, M. Dineva, Y. Chua, A. Ritchie, I. Ushiro-Lumb, C. Wisniewski, Simple amplification-based assay: a nucleic acid-based point-of-care platform for HIV-1 testing, J. Infect. Dis. (2010) S65–S71.
[39] M. You, M. Lin, S. Wang, X. Wang, G. Zhang, Y. Hong, Y. Dong, G. Jin, F. Xu, Three-dimensional quick response code based on inkjet printing of upconversion fluorescent nanoparticles for drug anti-counterfeiting, Nanoscale 8 (2016) 10096–10104.